Supporting Information

Table of Contents

1. Experimental Section

Materials and Instruments

Materials. Cyclen dimer **4**, chiral amide side chains (*R*)- and (*S*)-**5** were synthesized according to the reported method. $LnCl_3 \cdot 6H_2O$ and Cs_2CO_3 were purchased from Sigma-Aldrich Co. (St. Louis, USA). Solvents were purchased from Wako Pure Chemical Industries (Osaka, Japan) and Nakalai Tesque Inc. (Kyoto, Japan). Amino-modified silica gel (NH_2-SiO_2) for column chromatography was purchased from Fuji Silysia Chemical (Aichi, Japan).

Instruments. ^1H and $^{13}C\{^1H\}$ NMR spectra were recorded on a JEOL Lambda 400 spectrometer operating at 400 MHz for ^1H and 100 MHz for ^{13}C. Chemical shifts are reported in parts per million (δ) downfield from tetramethylsilane (TMS) for ^1H and a deuterated solvent for ^{13}C, respectively. IR spectra were recorded on a JASCO FT/IR-4100 type A spectrometer. Absorption spectra were measured using a 1-cm quartz cell on a JASCO V-670 spectrophotometer. CD spectra were measured using a 1-cm quartz cell on a JASCO J-820 spectropolarimeter. Luminescence spectra were recorded using a 1-cm quartz cell on a Perkin–Elmer LS-50B. Elemental analyses were performed at the Microanalytical Laboratory, Osaka City University.

Synthetic Procedures and Product Characterizations

Synthesis of (*R*)-**2** and (*S*)-**2**

General procedure: A mixture of **4**·4TFA (93 mg, 0.076 mmol), (*R*)-**5** (150 mg, 0.76 mmol) and Cs_2CO_3 (370 mg, 1.1 mmol) in acetonitrile (38 mL) was refluxed for 3 h. The solvent was removed by evaporation

and the residue was dissolved in CH_2Cl_2. After the removal of the insoluble material by filtration, the solvent was removed under reduced pressure. The obtained residue was purified by column chromatography (NH_2-SiO_2, CH_2Cl_2/MeOH 100:0 to 85:15), followed by reprecipitation (MeOH/ether) to afford **2b** as a white solid (69 mg, 0.046 mmol, 61%): mp 117 °C; $[\alpha]_D^{25}$=+57.1 (*c* 0.075 in MeOH); IR (KBr) ν 3302, 2929, 2819, 1656, 1527, 1110, 702 cm^{-1}; ^1H NMR ($CDCl_3$, 400 MHz): δ 7.93 (br s, 4H), 7.4–6.8 (m, 32H), 5.02 (m, 4H), 4.17 (br s, 8H), 3.1–2.3 (m, 48H), 1.47 (d, *J* = 7.0 Hz, 12H) ppm; ^{13}C NMR ($CDCl_3$, 100 MHz): δ 170.87, 169.88, 143.30, 139.05, 129.14, 128.86, 127.74, 127.67, 127.01, 126.31, 58.93, 58.72, 53.41, 52.75, 48.67, 42.95, 21.93 ppm; Anal. Calcd for $C_{80}H_{108}N_{16}O_8 \cdot 4(H_2O)$: C, 64.32; H, 7.83; N, 15.00. Found C, 64.86; H, 7.61; N, 15.25.

(*S*)-**2** was synthesized from **9**·4TFA and (*S*)-**5**: 52%, mp 117 °C; $[\alpha]_D^{25}$=–56.5 (*c* 0.075 in MeOH).

Synthesis of (*R*)-**2**Ln and (*S*)-**2**Ln

General procedure: (*R*)-**2** (37.2 mg, 0.0249 mmol) and $EuCl_3 \cdot 6H_2O$ (18.2 mg, 0.0497 mmol) was dissolved in a mixed solvent of methanol (2 mL) and water (2 mL). After the removal of solvent by distillation, the obtained residue was purified by reprecipitation (MeOH/Et_2O) to afford (*R*)-**2**Eu as a white solid (45.1 mg, 0.0204 mmol, 82%), Anal. Calcd for $C_{80}H_{108}N_{16}O_8 \cdot 2(EuCl_3) \cdot 16(H_2O)$: C, 43.15; H, 6.34; N, 10.06. Found C, 42.80; H, 6.27; N, 10.17.

(*S*)-**2**Eu was synthesized from (*S*)-**2** and $EuCl_3 \cdot 6H_2O$: 52%, Anal. Calcd for $C_{80}H_{108}N_{16}O_8 \cdot 2(EuCl_3) \cdot 16(H_2O)$: C, 43.15; H, 6.34; N, 10.06. Found C, 42.93; H, 6.11; N, 10.19.

(*R*)-**2**Tb was synthesized from (*R*)-**2** and $TbCl_3 \cdot 6H_2O$: 70%, Anal. Calcd for $C_{80}H_{108}N_{16}O_8 \cdot 2(TbCl_3) \cdot 18(H_2O)$: C, 42.20; H, 6.38; N, 9.84. Found C, 42.13; H, 6.19; N, 9.84.

(*S*)-**2**Tb was synthesized from (*S*)-**2** and $TbCl_3 \cdot 6H_2O$: 78%, Anal. Calcd for $C_{80}H_{108}N_{16}O_8 \cdot 2(TbCl_3) \cdot 18(H_2O)$: C, 42.20; H, 6.38; N, 9.84. Found C, 42.35; H, 6.29; N, 9.70.

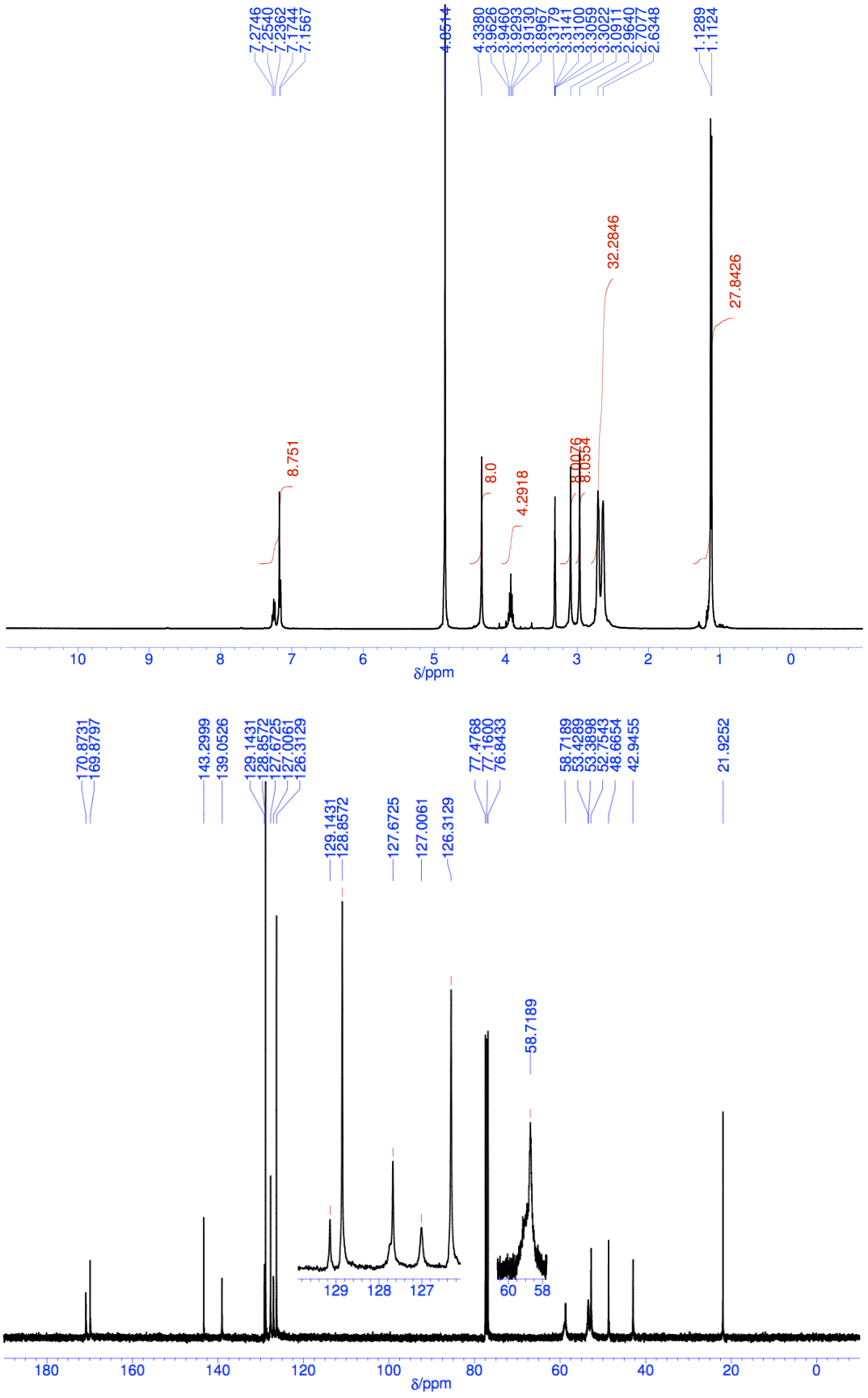

Fig. S1. ^{1}H and ^{13}C NMR spectra of (*R*)-**2** ($CDCl_3$, rt).

2. Supplemental Figures

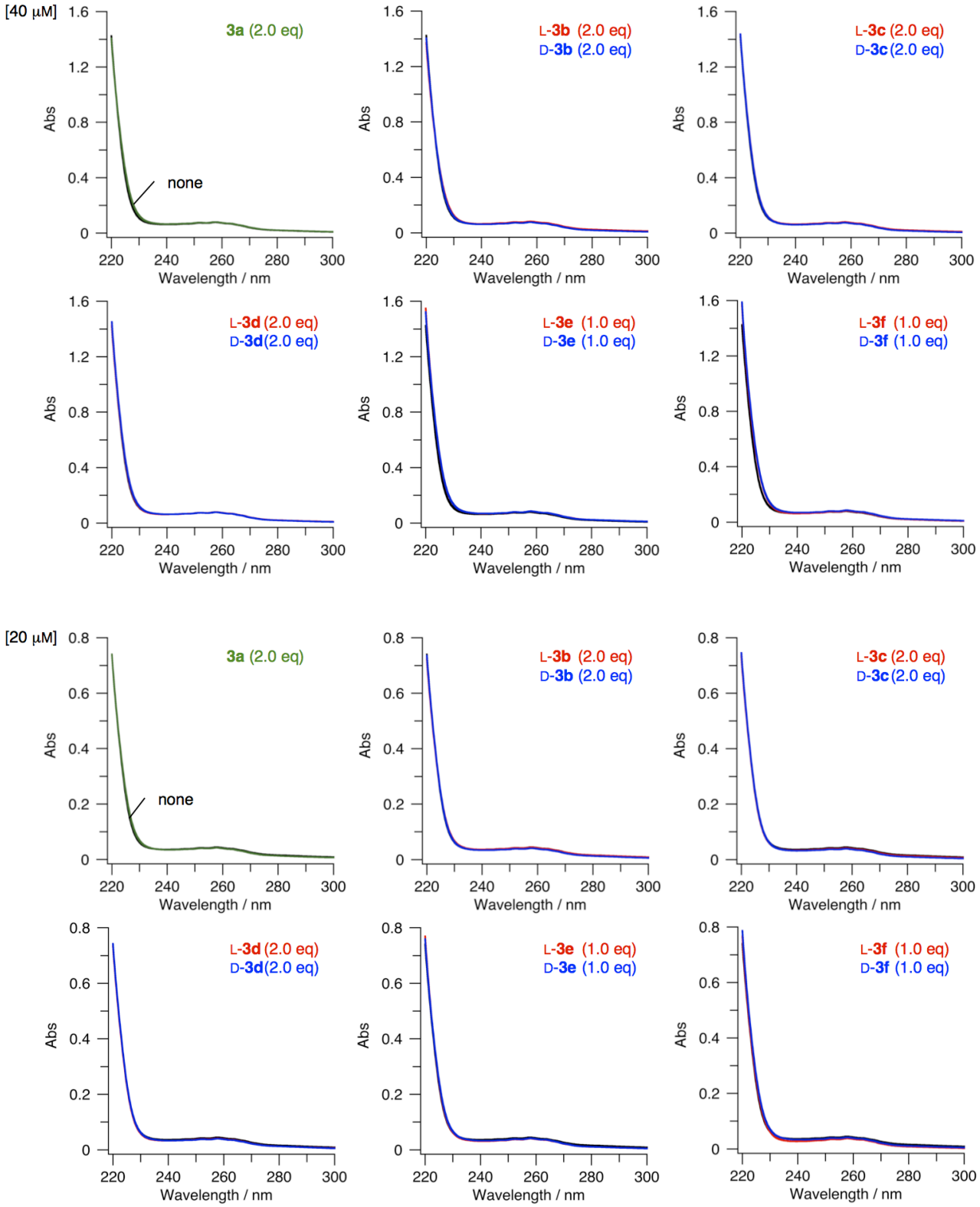

Fig. S2. Absorption spectra of (*R*)-**2**Eu (top: 40 μM, bottom: 20 μM) with DCHA (2.0 eq) and various amino acids (**3a–d**: 2.0 eq, **3e**,**f**: 1.0 eq) in MeOH (rt, 1 cm quartz cell).

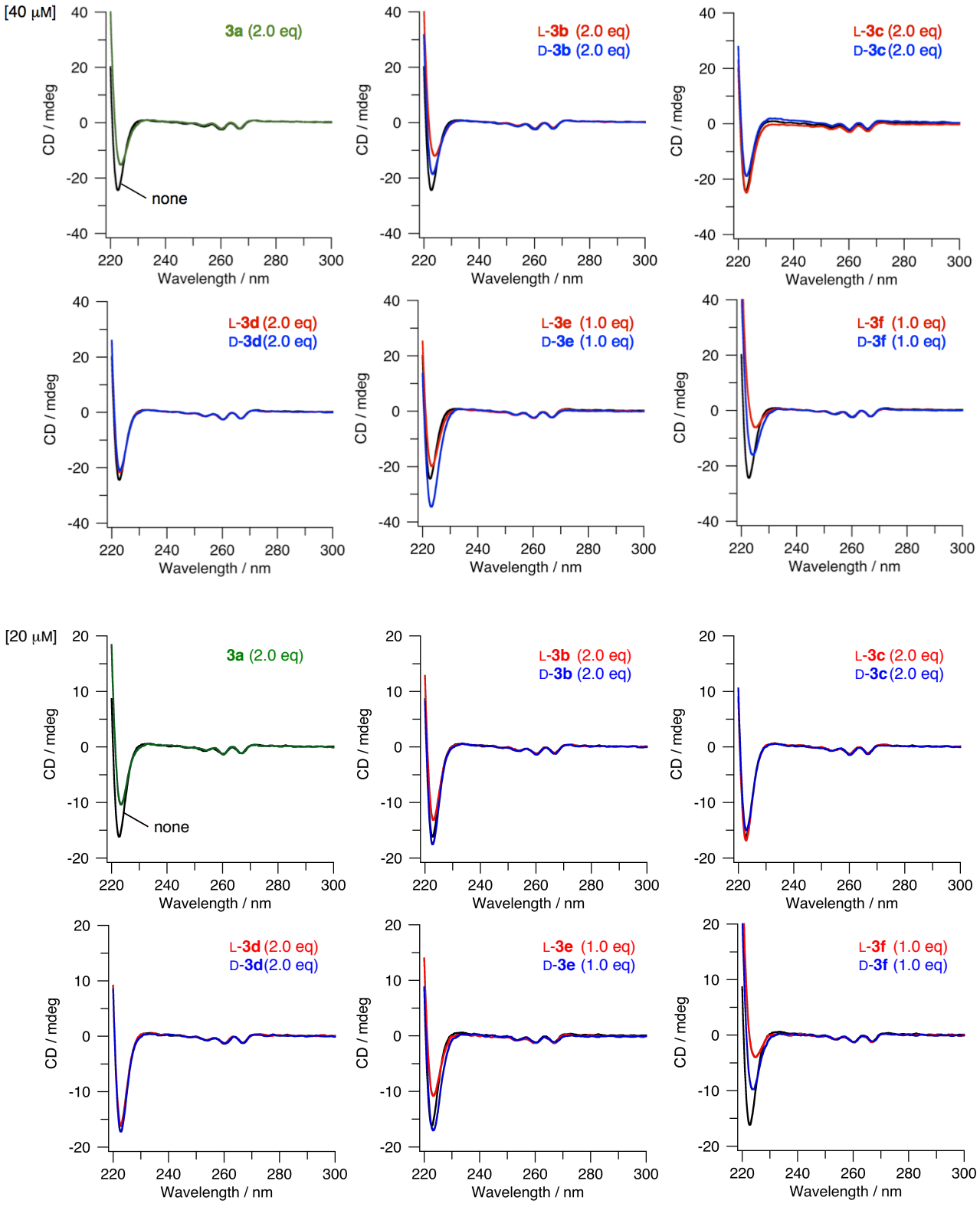

Fig. S3. CD spectra of (*R*)-**2**Eu (top: 40 μM, bottom: 20 μM) with DCHA (2.0 eq) and various amino acids (**3a**–**d**: 2.0 eq, **3e**,**f**: 1.0 eq) in MeOH (rt, 1 cm quartz cell).

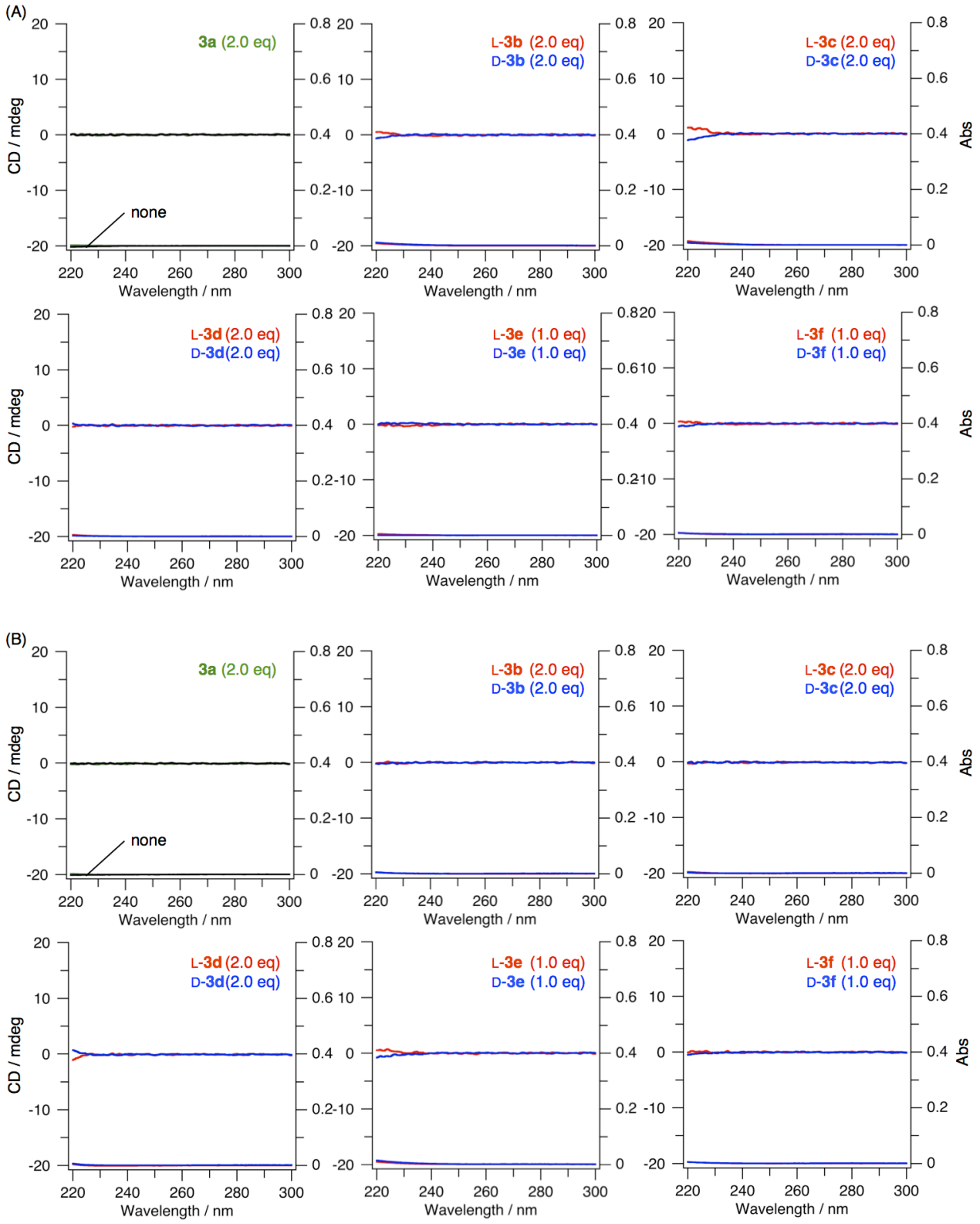

Fig. S4. Absorption and CD spectra of *N*-Boc-amino acids without (A) and with DCHA (B) in MeOH. (**3a**–**d**: 40 μM, **3e**,**f**: 20 μM, DCHA: 40 μM) in MeOH (rt, 1 cm quartz cell).

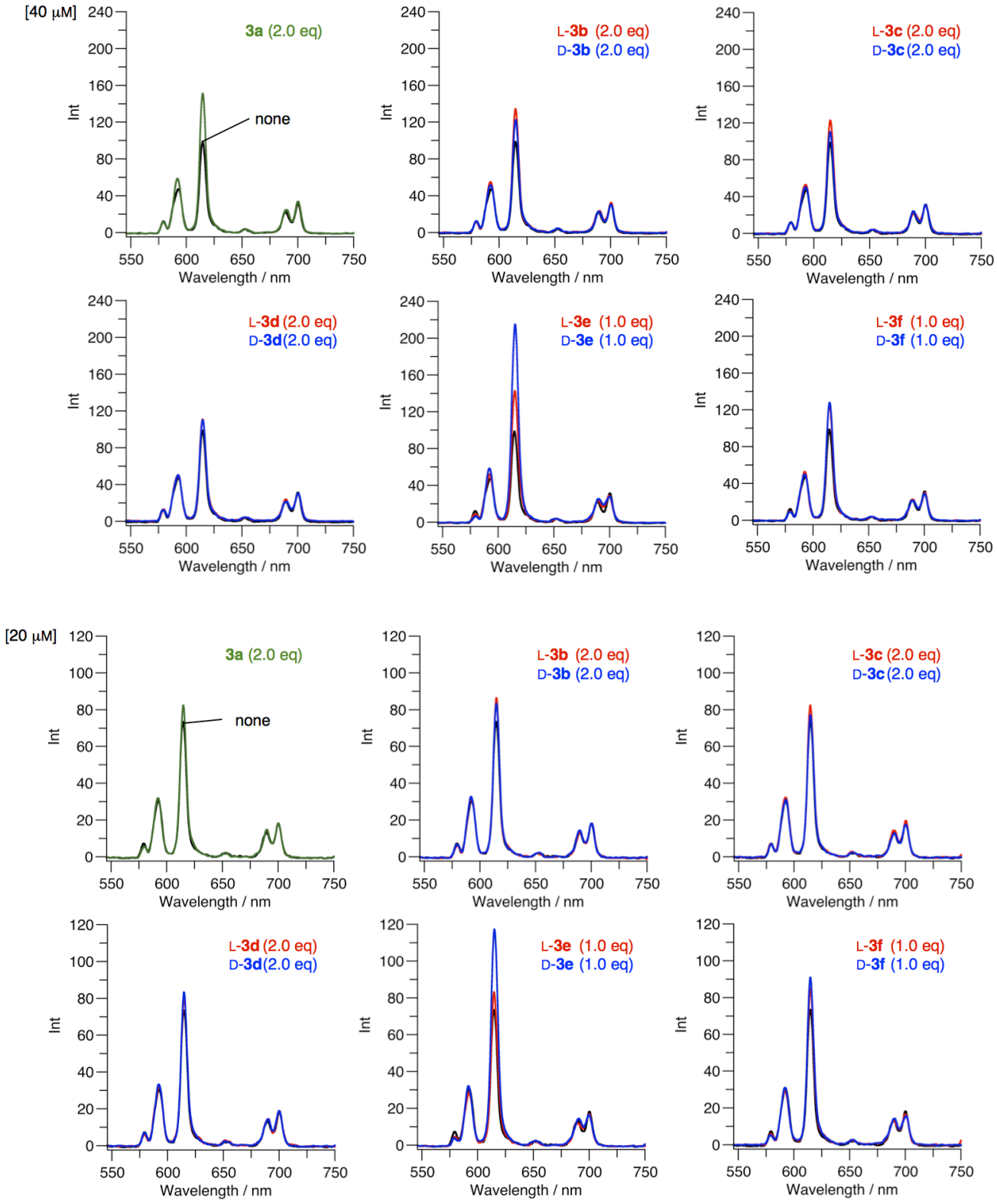

Fig. S5. Luminescent spectra of (*R*)-**2**Eu (top: 40 μM, bottom: 20 μM) with DCHA (2.0 eq) and various amino acids (**3a**–**d**: 2.0 eq, **3e**,**f**: 1.0 eq) in MeOH (rt, 1 cm quartz cell, λ_{ex} = 254 nm, slit: 10 nm / 5 nm).

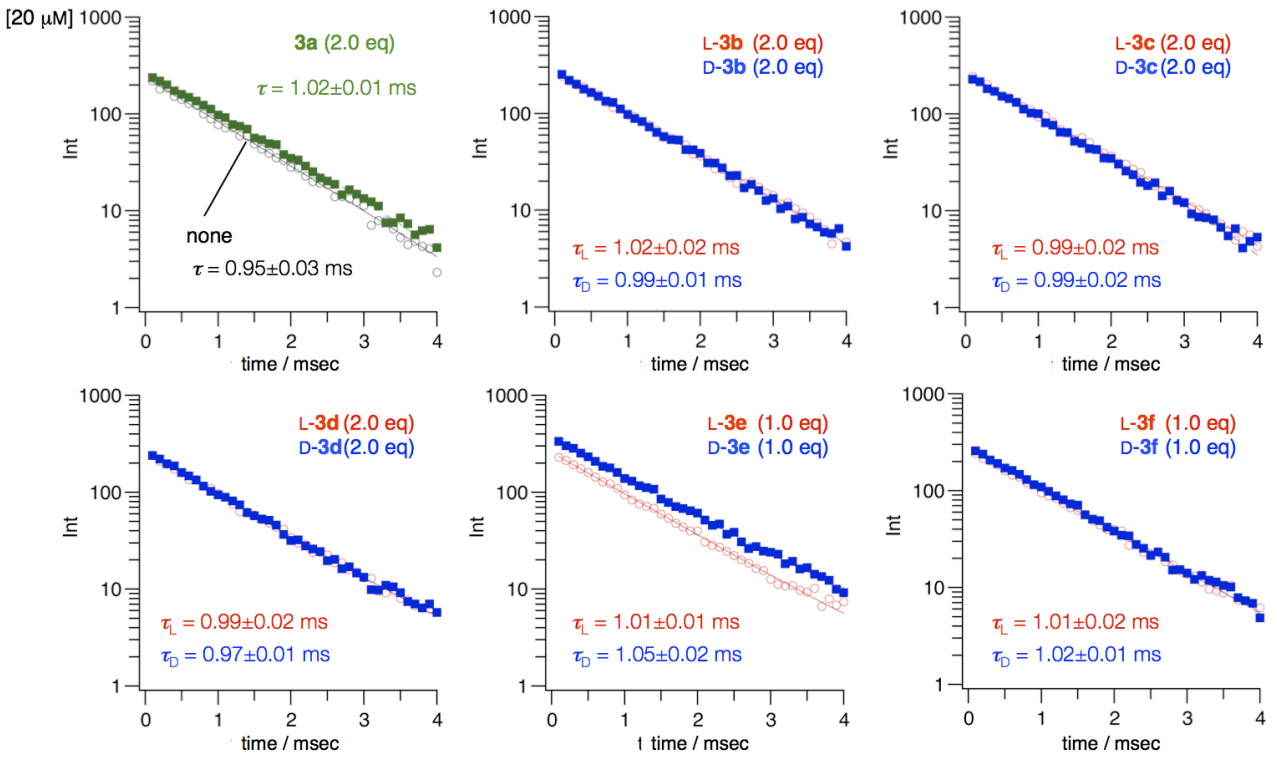

Fig. S6. Time decay spectra of (*R*)-**2**Eu (20 μM) with DCHA (2.0 eq) and various amino acids (**3a–d**: 2.0 eq, **3e**,**f**: 1.0 eq) in MeOH (rt, 1-cm quartz cell, λ_{ex} = 254 nm, λ_{em} = 615 nm, slit: 10 nm / 10 nm).

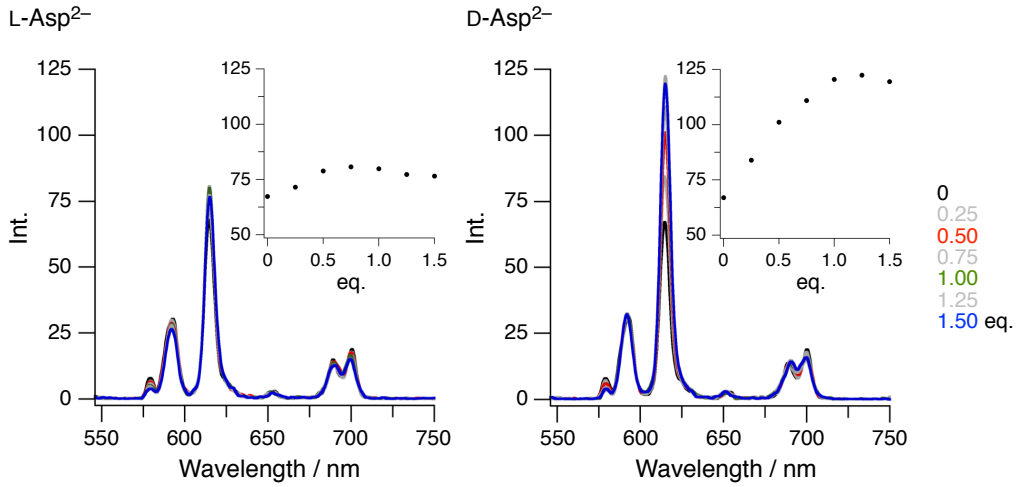

Fig. S7. Plots of luminescent intensity of (*R*)-**2**Eu (20 μM) with **3e**·DCHA (0–1.5 eq, λ_{em} = 615 nm) in MeOH (rt, 1 cm quartz cell, λ_{ex} = 254 nm, slit: 10 nm / 5 nm).

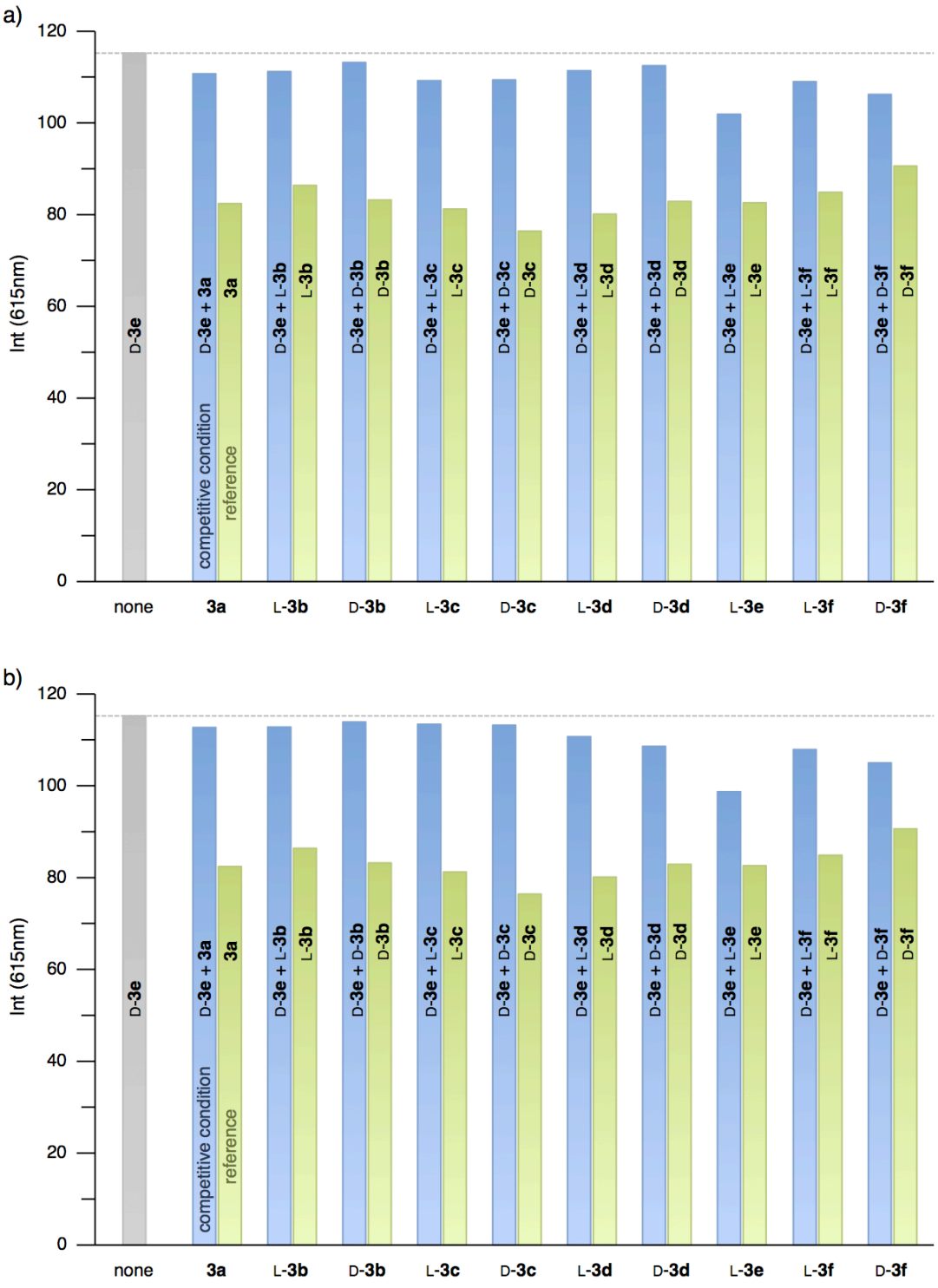

Fig. S8. Luminescence intensity (615 nm) of (*R*)-**2**Eu (20 μM) with DCHA (2.0 eq) and various amino acids (**3a**–**f**) in MeOH under competitive condition (**3a**–**d**: 2.0 eq, **3e**,**f**: 1.0 eq). a) No additional DCHA. b) Additional DCHA (2.0 eq).

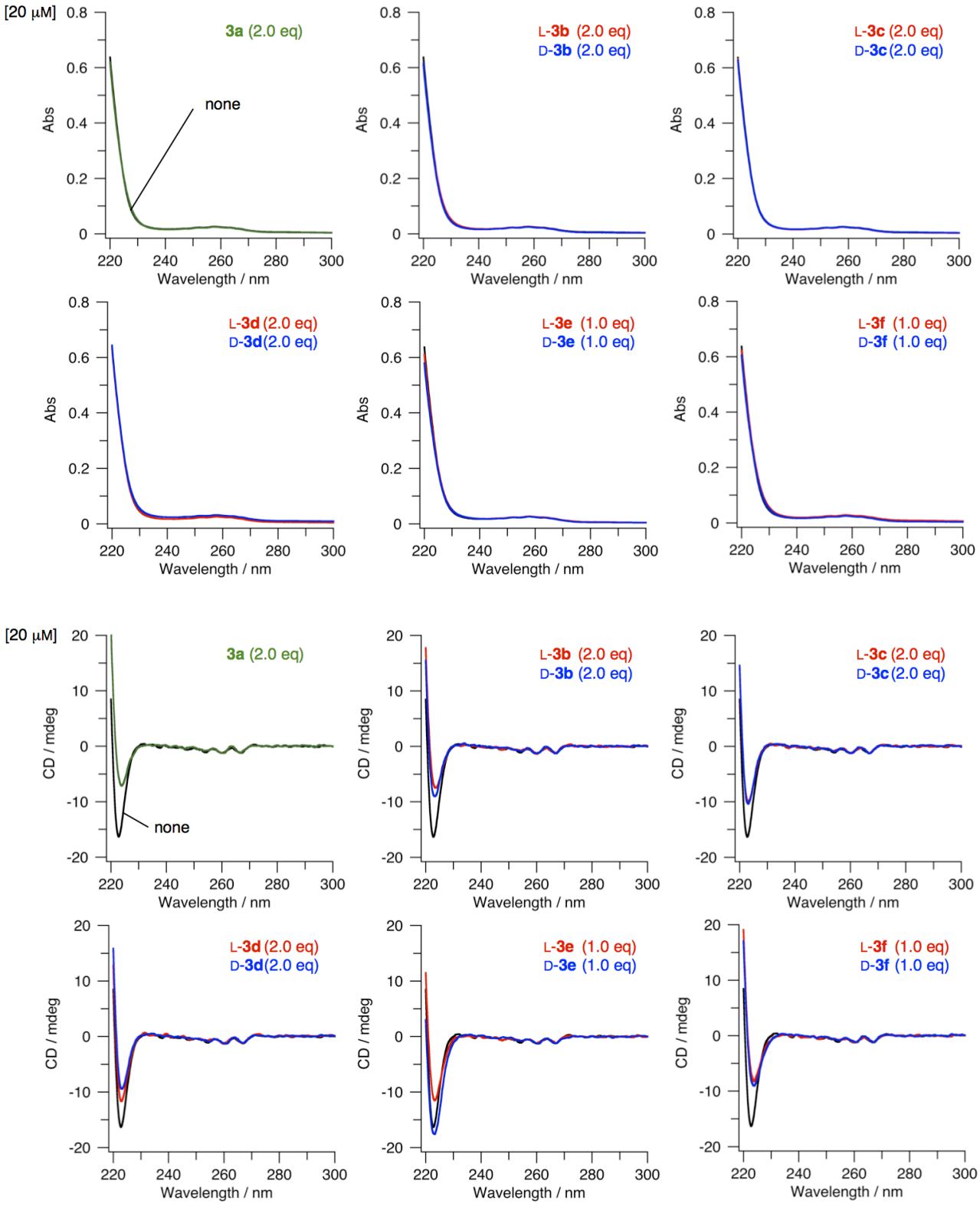

Fig. S9. Absorption (top) and CD (bottom) spectra of (*R*)-**2**Tb (20 μM) with DCHA (2.0 eq) and various amino acids (**3a**–**d**: 2 eq, **3e**,**f**: 1.0 eq) in MeOH (rt, 1-cm quartz cell).

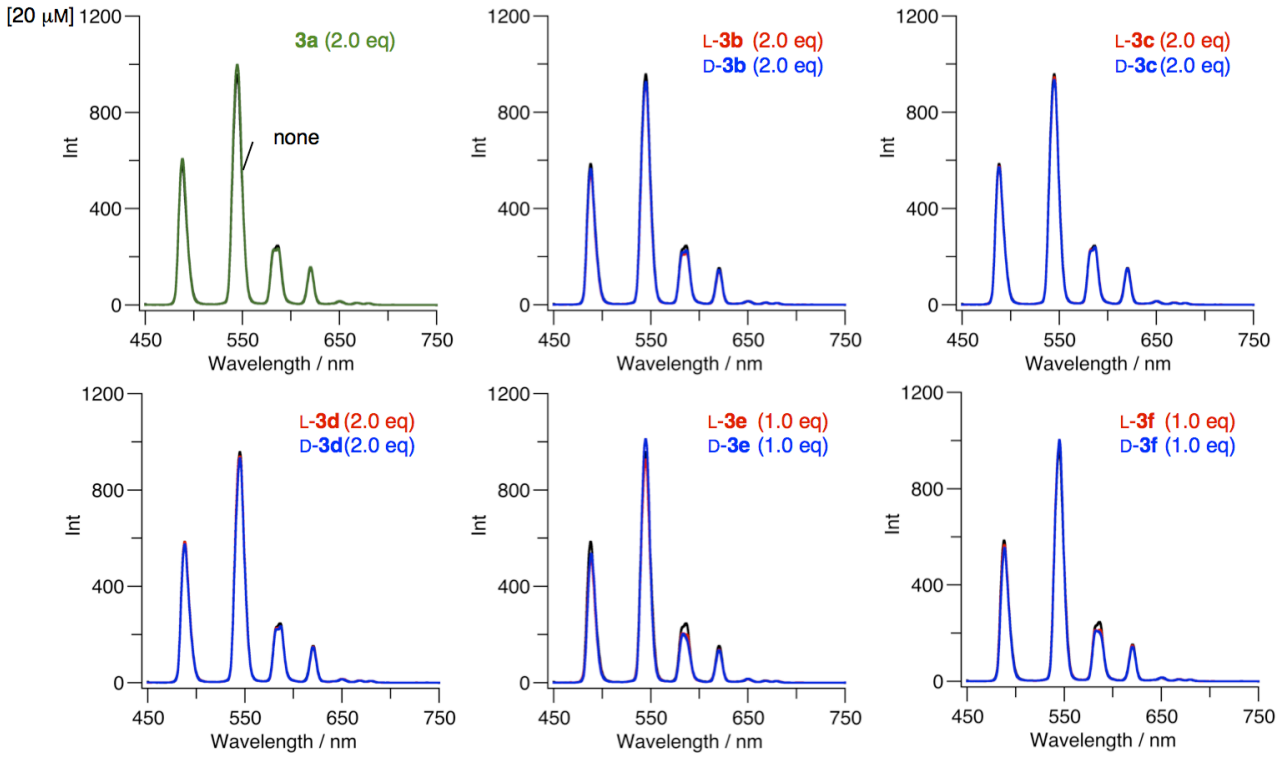

Fig. S10. Luminescent spectra of (*R*)-**2**Tb (20 μM) with DCHA (2.0 eq) and various amino acids (**3a**–**d**: 2.0 eq, **3e**,**f**: 1.0 eq) in MeOH (rt, 1 cm quartz cell, λ_{ex} = 254 nm, slit: 10 nm / 5 nm).

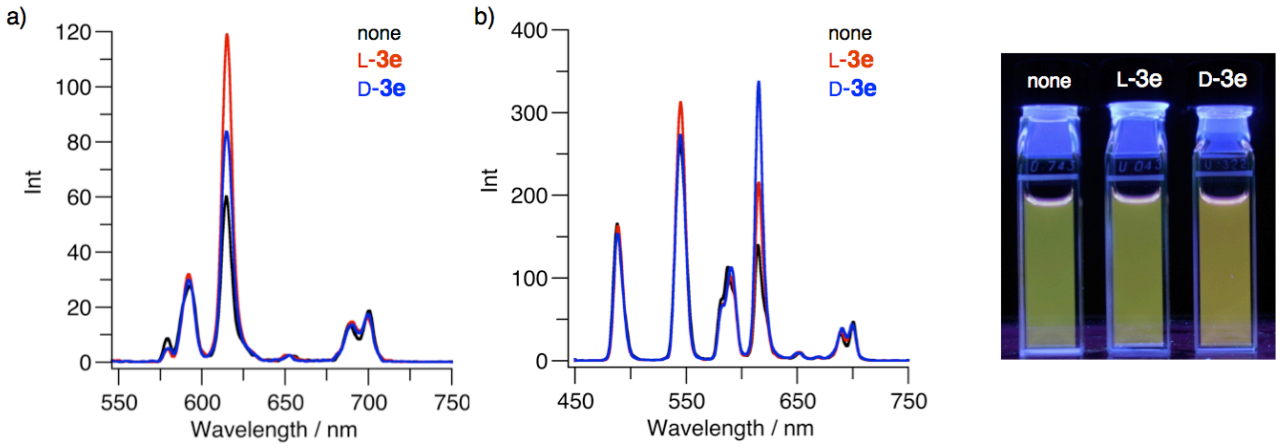

Fig. S11. a) Luminescent spectra of (*S*)-**2**Eu (20 μM) with DCHA (2.0 eq) and **3e** (1.0 eq) in MeOH (rt, 1 cm quartz cell, λ_{ex} = 254 nm, slit: 10 nm / 5 nm). b) Luminescent spectra of (S)-(*R*)-**2**Eu (80 μM) and (*S*)-**2**Tb (8 μM) with D/L-3e (88 μM) and DCHA (176 μM) in MeOH (rt, 1 cm quartz cell, λ_{ex} = 254 nm, slit: 10 nm / 5 nm) (left) and naked eye detection of the luminescence excited by UV lamp (λ_{ex} = 254 nm) (right).

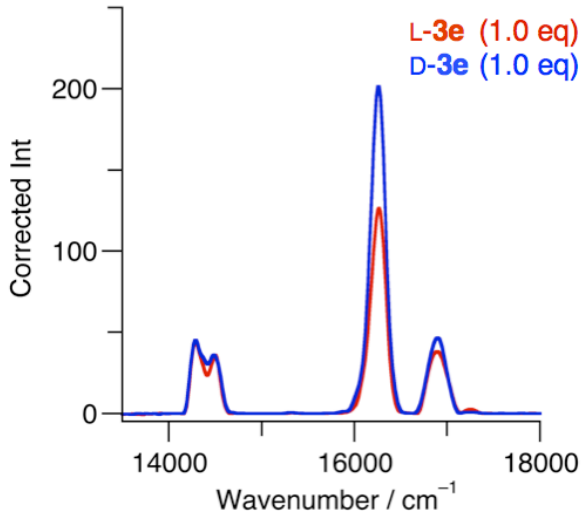

Fig. S12. Corrected luminescent spectra of (*R*)-**2**Eu (20 μM) with DCHA (2.0 eq) and **3e** (1.0 eq) in MeOH (rt, 1 cm quartz cell, λ_{ex} = 254 nm, slit: 10 nm / 5 nm).

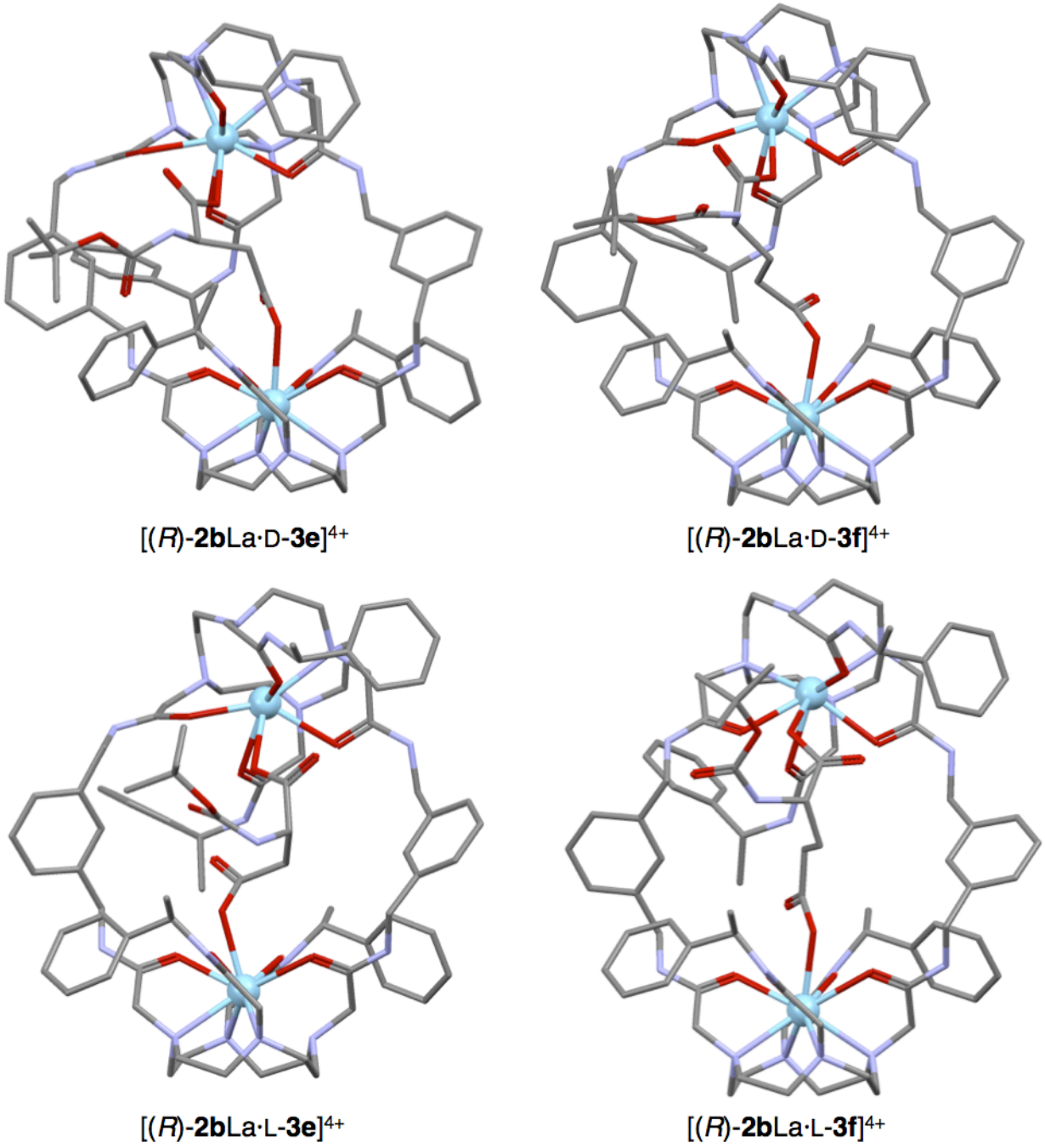

Fig. S13. Molecular mechanics modeling of (*R*)-**2**La·D-**3e** and (*R*)-**2**Eu·L-**3e**, (*R*)-**2**Eu·D-**3f** and (*R*)-**2**Eu·L-**3f**.